

Potential of Near-Field Microwave Imaging in Breast Cancer Detection Utilizing Tapered Rectangular Waveguide Probes

Wael Saleh and Nasser Qaddoumi

Microwave Imaging & Nondestructive Evaluation Lab. (minel)
Electrical Engineering Department, School of Engineering
American University of Sharjah
P. O. Box: 26666, Sharjah, UAE
Fax: (971)-6515-2979, Phone: (971)-6515-2933
nqaddoumi@aus.edu

Abstract — Microwave imaging for medical applications has been of interest for many years. A novel microwave noninvasive testing technique is presented for breast cancer detection. The physical basis for breast tumor detection with microwave imaging is the contrast in dielectric properties of normal and malignant breast tissues. A method adopting Fourier Transform Matching (FTM) technique and utilizing the reflection coefficient at the aperture of a tapered rectangular waveguide sensor radiating into a breast is described resulting in microwave images that indicate the presence of a tumor. These images demonstrate the feasibility of detecting breast tumors using this approach.

Index Terms — biomedical electromagnetic imaging, cancer, electromagnetic reflection, microwave imaging, microwave measurements, rectangular waveguide probe, tumors.

I. INTRODUCTION

Non-destructive and non-invasive testing methods exploiting microwave sensors and probes for the intention of material examination are quite well established and have been applied to several media [1-10]. The increased use of composite materials for industrial, medical, and military applications presents quite a challenge to many non-destructive and non-invasive testing methods. Difficulties arise from the inherent anisotropy and physical property heterogeneities of these materials, as well as the relative high absorption and scattering of the radiated signals. The success achieved and the promising results obtained when utilizing near-field microwave non-destructive testing techniques in wide range of industrial applications such as corrosion detection, laminated composite inspection, surface crack detection and material characterization led researchers to adopt near-field microwave imaging for medical applications such as breast cancer detection [4-10]. The spread of breast cancer worldwide and the need for new technologies to improve breast cancer detection present a challenge to the standard medical screening methods. Tumor detection, in the early stages, is crucial if patients are to be treated effectively and with minimally invasive

procedures. Thus, any technique that can improve on, or add to, existing breast tumour detection methods is welcome. Recently, microwave imaging and noninvasive testing has been applied to the detection of breast cancer [11-17].

The physical basis for tumor detection with microwave imaging and noninvasive testing techniques is the high contrast in dielectric properties between normal and malignant breast tissues. Near-field microwave noninvasive testing and evaluation (NIT&E) techniques can be a successful candidate for the detection of breast cancer because of their demonstrated potential in dealing with dielectric materials [8]. Near-field microwave NIT&E techniques are accomplished by transmitting an electromagnetic wave at a relatively high frequency towards a structure. The magnitude and/or phase information of the reflected wave properties are measured to obtain information about the composition and the integrity of the structure.

II. THEORETICAL BACKGROUND

Modeling the interaction between electromagnetic waves and multilayer dielectric media such as the breast is essential for tumor detection. Breast is made of layers, skin and tissue. The E-plane tapered waveguide is one whose opening is flared in the direction of the E-field as shown in Fig. 1. The narrow side of a rectangular waveguide, of cross-section $a \times b$, is flared from breadth b to breadth d in a taper of radial length ρ . The broad side, a , is constant. The semi-angle of the taper is Φ , and the distance between the waveguide aperture and taper aperture is L . We will consider a general stratified structure of any number of dielectric layers (N) in front of the tapered rectangular waveguide as shown in figure 1. The n^{th} layer has complex relative dielectric constant ϵ_m and thickness d_n . Once irradiated by a microwave signal, the electric field in each layer may be expressed in terms of the media constitutive parameters for any stratified dielectric media terminated with a dielectric infinite half-space. Fourier Transform matching technique will be utilized to express the

electric field in a recursive model. Once the field coefficients are obtained, theoretical images can be formed by calculating the reflection coefficient at each scanned point. A tapered rectangular waveguide with dominant mode excitation (TE₁₀) is used to illuminate the breast with electromagnetic waves at microwave frequencies. The waveguide aperture lies in the *xy*-plane and is centered at the origin. The breast is placed in the near-field region of the tapered rectangular waveguide. The intention is to find the electric field's coefficients in each layer.

For TE₁₀ mode, the excitation aperture fields are,

$$\overline{E}_{ap}(x, y) = \hat{y}Q \cos\left(\frac{\pi}{a}x\right) e^{-j\frac{ky^2}{2L}} \quad (1)$$

$$\overline{H}_{ap}(x, y) = \hat{x}\frac{Q}{\eta} \cos\left(\frac{\pi}{a}x\right) e^{-j\frac{ky^2}{2L}} \quad (2)$$

$$\text{Where } Q = j A_1 \sqrt{\frac{2}{\pi k \rho}} e^{-jk\rho}, L = \rho \cos(\phi)$$

$k = 3.336 \times 10^{-9} \omega \sqrt{\mu_{rf} \epsilon_{rf}}$ 1/m is the propagation constant, A_1 is the complex reflection coefficient, μ_{rf} and ϵ_{rf} are the relative permeability and permittivity of the material filling the guide, ω is the radian frequency rad/s, and finally, $\eta = 376.73 \sqrt{\mu_{rf} / \epsilon_{rf}} \Omega$ is the intrinsic impedance of the filling material [18].

The phase term $e^{j(ky^2/2L)}$ in equations (1) and (2) describes the spatial phase distribution over the aperture as a function of the coordinate *y*. It shows that the phase of the field at the aperture of the tapered waveguide is not uniform as in the case of the conventional rectangular waveguide. It actually highlights the fact that the phase is in quadrature relation with *y*. By comparing the tapered waveguide fields to the conventional rectangular waveguide field, the influence of the tapering can be observed in both magnitude and phase of the aperture fields. This indicates that the radiation pattern will also vary leading to a change in obtained images.

To model the interaction between the breast and the electric field, we need first to calculate the electric field distribution at every coordinate point (*x, y, z*). This requires finding field coefficients in each layer of the structure. Starting from Maxwell's equations, we can obtain the field solution by applying the Fourier Transform technique. This involves expanding the field in each layer in terms of the Fourier Integrals and applying boundary conditions at each interface. Having the solution for the field in the first layer, the reflection coefficient is calculated from the effective admittance at the waveguide's aperture [19-20]. The normalized admittance at the waveguide aperture is written as:

$$Y_s(x, y) = \frac{j}{4\pi^3 \omega \mu Y_0 \sin(\frac{\pi x}{a})} \bullet \left. \begin{aligned} & \left\{ \int_{-\infty}^{\infty} \int_{-\infty}^{\infty} \frac{C_{11} I^*}{1 + g_{11}} (-1 + g_{11}) e^{j(k_x x + k_y y)} dk_x dk_y, \dots : x \in [x_1, x_2], y \in [y_1, y_2] \right\} \\ & \left\{ \int_{-\infty}^{\infty} \int_{-\infty}^{\infty} \frac{C_{12} I^*}{1 + g_{12}} (-1 + g_{12}) e^{j(k_x x + k_y y)} dk_x dk_y, \dots : \text{otherwise} \right\} \end{aligned} \right\} \quad (3)$$

The detailed expressions of the constants involved in this equation are given in [19-20]. The reflection coefficient is given by:

$$\Gamma = \frac{1 - Y_s}{1 + Y_s} \quad (4)$$

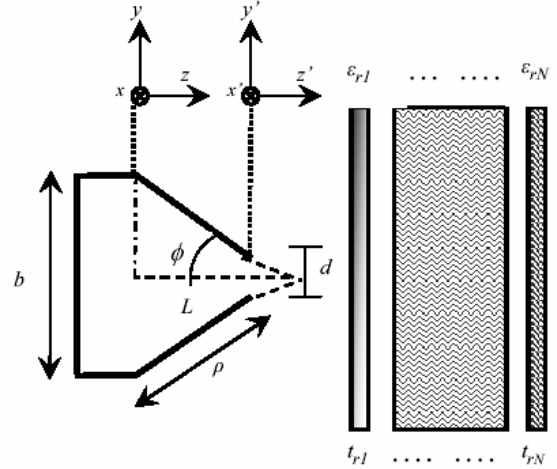


Fig. 1. The cross-section of an E-plane tapered rectangular waveguide radiating into an N-layer structure backed by free-space.

III. IMAGE FORMATION

From the microwave imaging point of view, a subsurface inclusion/defect is announced by a change in the complex dielectric constant of the layer in which the inclusion exists. The purpose of the microwave imaging system is to map this change spatially in 2-D image. The imaging mechanism is based on the basic idea that microwaves, once they are launched into a media, are very sensitive to discontinuities in the material space. In our case, the discontinuity is realized as a tumor in the breast tissue. The discontinuity causes some of the incident waves to reflect back toward the transmitter, and the remaining portion is transmitted forward into the structure. The power and the phase properties of the forward and backward traveling waves contain valuable information about the tumor (inclusion) the incident wave experienced. The phase and power properties are inferred from the measured complex reflection coefficient. An open-ended rectangular waveguide probe, tapered or standard, is utilized to measure the reflection coefficient in a certain imaging plane as a function of the spatial coordinates and outputs that as 2-D intensity image. Depending on the measurement

parameter, two types of images can be obtained, magnitude and phase images. The magnitude images are those formed by measuring the magnitude of the reflection coefficient (or a signal proportional to it) at the scanned point. In the phase images the contrast level is proportional to the phase of the reflection coefficient in the plane of imaging (xy -plane) [19-20].

IV. SIMULATION ANALYSIS

The breast model used in this investigation consists of breast tissue ($\epsilon_r = 9$ and $\sigma = 0.4$ S/m) of 60 mm thickness surrounded by an outer layer of skin ($\epsilon_r = 36$ and $\sigma = 4$ S/m) of 2 mm thickness. A tumor ($\epsilon_r = 50$ and $\sigma = 4$ S/m) of finite dimensions is presented within the breast tissue [19-20]. The waveguide is centered at the origin with its board dimension (a) along the x -axis and the narrow dimension (d) along the y -axis. We assume TE_{10} excitation mode for the waveguide with propagation in the z -direction. The breast might be terminated by an infinite half-space (IHS) of air or a conductor sheet (CS). All the theoretical investigations are conducted for an infinite half-space of air termination because the breast is classified as high lossy material and few portion of the microwave signal will reach the termination point. In addition, it is more comfortable for the patient because the metallic sheet is not attached to the breast and thus breast compression is avoided. Reflection coefficient has a phase and magnitude associated with it. The simulation results include the radiation patterns and the reflection coefficient. The radiation patterns are presented as the magnitude of the normalized electric field and real power patterns. The field distributions are obtained with steps of 0.1 mm, 0.1a, and 0.1b in the z , x , and y directions, respectively. The magnitude of the radiated field is either normalized for the electric field or in decibels (dB) for the radiated power.

Figure 3 shows the normalized electric field pattern in the yz -plane ($x = a/2$ plane) for 5 mm tumor depth. The fields are confined within the aperture's d -dimension up to a long distance inside the breast (around 5 mm) till they meet the tumor. Although, the tangential electric field is continues along the interfaces between the different layers, the normal component is not. The discontinuity depends on the ratio of the relative dielectric constant of each layer. This is shown clearly in Figure 3 between skin layer and the breast tissue layer since the contribution of the normal component of the electric field to the total electric field in this plane is more than that of the tangential component. Figure 4 shows the real power pattern in the yz -plane ($x = a/2$ plane) for 5 mm tumor depth. The real power dropped 10 dB below its maximum (at the aperture) at a distance of 2 mm from the aperture; in other words, when the microwaves started penetrating the breast tissue. At $z =$

5 mm and due to the presence of tumor, the real power again dropped 20 dB below its maximum (at the aperture).

To demonstrate the potential of the theoretical image formation capability on the optimization process, Figures 5 and 6 show the magnitude and phase images for a $6 \times 6 \times 3$ mm tumor 5 mm deep, respectively. These images are obtained using an X-band tapered rectangular waveguide loaded with a dielectric material ($\epsilon_r = 12.25$) operating at frequency of 3 GHz. The resolution in x and y directions is 1 mm. The magnitude image has a dynamic range of 0.7 and phase image has 3° degrees. The presence of the tumor is clearly visible. Also, the resolution of the images is high such that the xy dimensions of the tumor can be estimated directly from the image. Effects of the waveguide's radiation pattern (side lobes, beamwidth, etc.) are also indicated on the images.

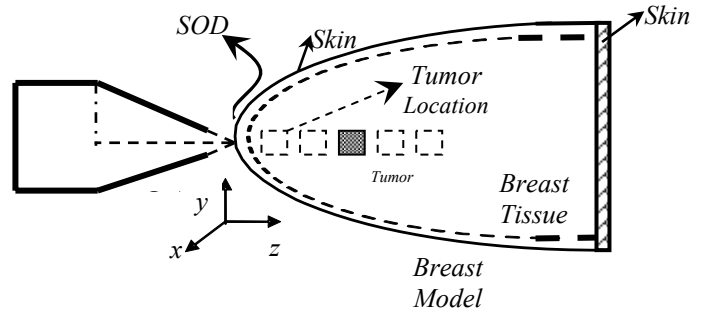


Fig. 2. Breast model with tumor embedded at different depths in front of the tapered rectangular waveguide sensor.

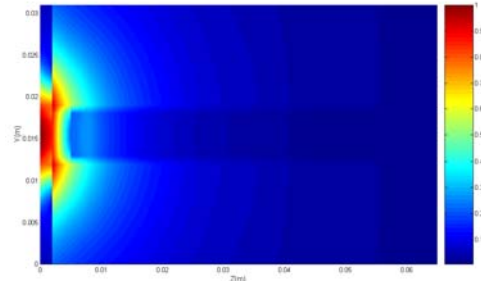


Fig. 3. Normalized electric field pattern of the breast with $6 \times 6 \times 3$ mm³ tumor at 5 mm depth at 3.0 GHz.

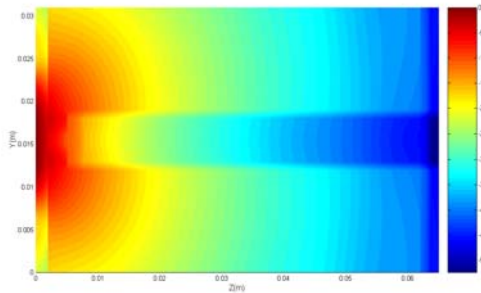


Fig. 4. Real power pattern (dB) of the breast with $6 \times 6 \times 3$ mm³ tumor at 5 mm depth at 3.0 GHz.

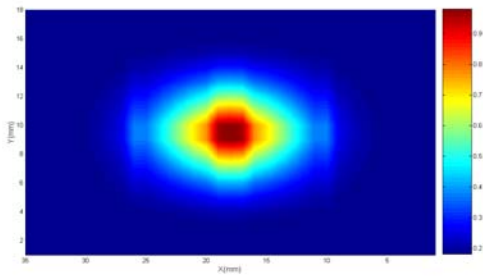


Fig. 5. Magnitude image of the breast with 6x6x3 mm³ tumor at 5 mm depth at 3.0 GHz.

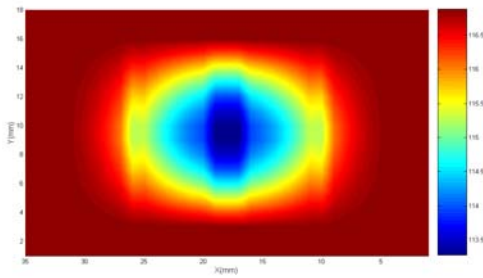


Fig. 6. Phase image of the breast with 6x6x3 mm³ tumor at 5 mm depth at 3.0 GHz.

V. CONCLUSIONS

Radiation patterns and theoretical images of magnitude and/or phase of reflection coefficient for different tumor depths at optimum operating frequency were obtained. The simulations presented verified the successful possibility of implementing the developed image formation model practically. There is still a massive amount of research and development to be conducted in order to achieve good performance. Current and in-progress measurements of dielectric properties of normal breast tissue and classic abnormalities will grant a solid base for the improved design of microwave imaging systems. In addition, microwave sensors will be increasingly operated at millimeter-wave frequencies and combined with other types of sensors (such as optical sensors, ultrasound sensors, etc.) in what so called “sensor fusion” or “multi-sensor data fusion” to provide greater sensitivity and discrimination

REFERENCES

- [1] Bahr, A. , R. Zoughi, and N. Qaddoumi, "Nondestructive Evaluation: Theory, Techniques, and Applications" Chapter on Microwave Techniques, An undergraduate introductory text on NDE, pp. 645-720, edited by P.J. Shull and M.J. Ehrlich, Marcel and Dekker, Inc. Publishers, April 2002.
- [2] Belhadj-Tahar, N.-E., A. Fourrier-Lamar, and H. de Chanterac, “Broad Band Simultaneous Measurement Of Complex Permittivity And Permuability Using A Coaxial Discontinuity,” *IEEE Trans. on Microwave Theory Tech.*, vol. MTT-38, pp. 1-7, Jan. 1990.
- [3] Decreton, M. C., and F. E. Gardiol, “Simple Non-Destructive Method for Measurement of Complex Permittivity,” *IEEE Trans. on Instrumentation and Measurement*, vol. IM-23, pp. 434-438, Dec. 1974.
- [4] Venugopalan, P., k. Jose, K. Nair, P Chaturvedi, and V. Ravindran, “Microwave Technique for Locating Inhomogenities in Cured Rocket Propellant Samples”, *NDT International*, 19(6), pp. 395-397, Dec. 1986.
- [5] Zoughi, R. and S. Bakhtiari, “Microwave Nondestructive Detection and Evaluation of Disbonding and Delamination in Layered-dielectric Slabs,”*IEEE Trans. on Inst. and Meas.*, 39(6), pp. 1059-1063, Dec. 1990.
- [6] Yeh, C. and R. Zoughi, “A Novel Microwave Method for Detection of Long Surface Cracks in Metals,” *IEEE Transactions on Instrumentation and Measurement*, vol. 43, no. 5, pp. 719-725, October, 1994.
- [7] Qaddoumi, N., S. Ganchev, G. W. Carriveau and R. Zoughi, “Microwave Imaging of Thick Composites with Defects,” *Materials Evaluation*, vol. 53, no. 5, August 1995.
- [8] Qaddoumi, N., R. Zoughi and G.W. Carriveau, “Microwave Detection and Depth Determination of Disbonds in Low-Permittivity and Low-Loss Thick Sandwich Composites,” *Research in Nondestructive Evaluation*, vol. 8, no. 1, 1996.
- [9] Huber, C., H. Abiri, S. Ganchev and R. Zoughi, “Modeling of Surface Hairline Crack Detection in Metals Under Coatings Using Open-Ended Rectangular Waveguides,” *IEEE Transactions on Microwave Theory and Techniques*, vol. 45, no. 11, pp. 2049-2057, November 1997.
- [10] Huber, C., S.I. Ganchev, R. Mirshahi, J. Easter and R. Zoughi, “Remote Detection of Surface Cracks/Slots Using Open-Ended Rectangular Waveguide Sensors: An Experimental Investigation,” *Nondestructive Testing & Evaluation*, vol. 13, pp. 227-237, 1997.
- [11] S. C. Hagness, A. Taflove, and J. E. Bridges, “Two-Dimensional FDTD Analysis of a Pulsed Microwave Confocal System for Breast Cancer Detection: Fixed-Focus and Antenna-Array Sensors,” *IEEE Trans. Biomedical Engineering*, vol. 45, pp. 1470-1479, Dec. 1998.
- [12] S. C. Hagness, A. Taflove, and J. E. Bridges, “Three-Dimensional FDTD Analysis of a Pulsed Microwave Confocal System for Breast Cancer Detection: Design of an Antenna Array Element,” *IEEE Trans. Antennas Propagation*, vol. 41, pp. 783-791, May 1999.
- [13] E. C. Fear, and M. A. Stuchly, “Microwave Breast Cancer Detection.” *IEEE MTT-S Digest*, pp. 1037-1040, 2000.
- [14] X. Li and S. C. Hagness, “A Confocal Microwave Imaging Algorithm for Breast Cancer Detection,” *IEEE Microwave and Wireless Components Letters*, vol. 11, no. 3, pp. 130-132, March 2001.
- [15] E. Fear, S. C. Hagness, P. Meaney, M. Okoniewski, and M. Stuchly, “Enhancing Breast Tumor Detection with Near-Field Imaging,” *IEEE Microwave Magazine*, vol. 3, no. 1, pp. 48-56, March 2002.
- [16] Wael Saleh, David Wright, Philip Slade, and Nasser Qaddoumi, “Exploration of Breast Tumors Utilizing Noninvasive Near-Field Microwave Imaging,” *Conference on Precision Electromagnetic Measurements 2004*, 27 June - 2 July, London, UK.

- [17] Wael Saleh, Philip Slade, Nasser Qaddoumi, and David Wright, "Microwave Breast Cancer Detection Using Open-Ended Rectangular Waveguide Probes," *10th International Symposium on Microwave and Optical Technology*, August 22-25, 2005, Fukuoka, Japan.
- [18] Nasser Qaddoumi, Mohamed Abu-Khousa, and Wael Saleh, "Near-Field Microwave Imaging Utilizing Tapered Rectangular Waveguides," *IEEE Transactions on Instrumentation and Measurements*, vol.55, no. 5, pp. 1752-1756, October 2006.
- [19] Mohammed Abu-Khousa, Wael Saleh and Nasser Qaddoumi, "Defect Imaging and Characterization in Composite Structures Using Near-field Microwave Nondestructive Testing Techniques," *Journal of Composite Structures*, 62 (2003), pp. 255-259.
- [20] Wael Saleh, "Breast Cancer Detection Utilizing a Non-Invasive Harmless Near-Field Microwave Testing Technique," Poster for *the Britain's Top Younger Engineers Competition*, 14th December 2004, House of Commons, London, UK.
- [21] Wael Saleh, Philip Slade, Nasser Qaddoumi, and David Wright, "Microwave Breast Cancer Detection Using Open-Ended Rectangular Waveguide Probes," *Special Issue of the International Journal of Microwave and Optical Technology*, 2006 (accepted for publication).